Effect of Phosphorus Content on Cu/Ni-P/Sn-3.5Ag Solder Joint Strength after Multiple Reflows

ZHONG CHEN,[1,2] ADITYA KUMAR,[1] and M. MONA[1]

1.—School of Materials Science and Engineering, Nanyang Technological University, Singapore 639798. 2.—E-mail: aaszchen@btu.edu.sg

Electroless Ni-P layers with three different P contents (6.1 wt.%, 8.8 wt.%, and 12.3 wt.%) were deposited on copper (Cu) substrates. Multilayered samples of Sn-3.5Ag/Ni-P/Cu stack were prepared and subjected to multiple reflows at 250°C. A tensile test was performed to investigate the effect of P content on the solder joint strength. The low P samples exhibited the highest joint strength after multiple reflows, while the strength of medium and high P samples decreased more rapidly. From interfacial analysis, the Ni_3Sn_4 intermetallic compound (IMC) formed at the interface of low P sample was found to be more stable, while the one of medium and high P samples spalled into the molten solder. The IMC spallation sped up the consumption of electroless Ni-P, leading to the large formation of Cu-Sn IMCs. Fractographic and microstructural analyses showed that the degradation in solder joint strength was due to the formation of layers of voids and growth of Cu-Sn IMCs between the solder and the Cu substrate.

Key words: Electroless nickel, lead-free solder, interfacial reactions, intermetallic compounds (IMCs), mechanical strength

INTRODUCTION

Copper (Cu) has been extensively used as under bump metallization (UBM) and substrate metallization for flip-chip and ball-grid-array (BGA) packages. Yet, Cu-based metallization faces the problem of rapid Cu-Sn IMC growth due to the fast reaction between Sn and Cu. During the soldering process, Sn reacts rapidly with Cu at the liquid solder/Cu interface and forms a Cu-Sn intermetallic compound (IMC). The so-called IMC spallation, which describes the detachment of IMC from the underlying layer, has been reported to occur with Cu-based metallization.[1,2]

Several UBM systems have been developed and investigated. Ni-based metallizations have been identified as the preferred metallization over Cu to be used with Sn-rich solders. The main reason for this is the slow reaction of Ni with solder as compared to that of Cu.[3] Among Ni-based UBMs, electroless nickel has been employed for under bump and substrate metallizations due to its numerous advantages such as maskless selective deposition, low processing cost, good uniformity, good solderability, and excellent corrosion resistance.[4–6]

Electroless nickel plating with hypophosphite ($H_2PO_2^-$) as a reducing agent has been known to yield amorphous or nanocrystalline Ni-P alloys.[6] The presence of phosphorus makes the soldering reaction with Ni-P more complicated than the one with pure Ni. In the reaction between Sn-bearing solders and pure nickel, mainly one interfacial compound, Ni_3Sn_4 intermetallic, forms.[7] However, in the case of the Ni-P/solder reaction, at least three types of interfacial compounds, Ni_3Sn_4, Ni-Sn-P, and Ni_3P, form.[3–5,8–17] Other interfacial compounds such as Cu-Sn and Ni-Cu-Sn intermetallics have been also found to form in a few studies.[9,10] Because UBM/solder joint reliability is closely associated with the interfacial microstructure, it is important to understand the influence of P content on the mechanical properties of electroless Ni-P/solder joint.

Although the influence of P content on the mechanical properties of electroless Ni-P/solder joint has been investigated in a few studies,[11,12] different thicknesses of electroless Ni-P UBM were used for investigating and comparing the influence of P content on the joint strength. Recently, we have found[17] that the thickness of the electroless Ni-P layer itself influences the mechanical properties of the electroless Ni-P/solder joint. Thus, it is essential to separate the effect of electroless Ni-P thickness from the effect of P content. Accordingly, in this study, we used electroless Ni-P layers of different P contents but of the same thickness to investigate the effect of P content on the interfacial microstructure and

(Received March 10, 2006; accepted May 3, 2006)

tensile strength of the Cu/electroless Ni-P/Sn-3.5Ag solder joint.

In electronic manufacturing, at least two reflows are required. The first reflow forms an area of solder bumps on a chip surface, while the second reflow bonds the chip to a substrate. Multiple reflow, in fact, is often experienced during subsequent surface mount, testing, and repair. In the current study, multiple reflows up to 30 cycles were carried out. Our intention is to not only simulate the actual situation that a package may go through, but also to drive the interfacial reaction to the extreme condition to reveal the endurance limit of different Ni-P platings.

EXPERIMENTAL PROCEDURE

The Cu (99.99%) substrate of 6-mm thickness was used to fabricate the test samples for tensile testing. The Cu substrate was polished using 1-μm abrasive paper, and then ultrasonically cleaned with acetone for 10 min. Finally, it was etched with 20vol.%HNO_3 solution for a few seconds, followed by cleaning with deionized water. Electroless Ni-P was plated on cleaned Cu substrate in two steps. In the first step, the Cu surface was activated using the ruthenium-based commercial preinitiator. In the second step, electroless Ni-P was plated on the activated Cu surface using commercial electroless nickel solutions. After the electroless plating, a thin layer (~500 Å) of noncyanide immersion gold was deposited to protect the surface from oxidation. The P contents were 6.1 wt.%, 8.8 wt.%, and 12.3 wt.%, and will be referred to as low, medium, and high P subsequently. The Ni-P thickness was controlled to be around 3 μm for all three compositions so that the thickness effect on the tensile strength was eliminated.

For interfacial microstructure study, a thick layer (~350 μm) of Sn-3.5Ag solder was reflowed on the electroless Ni-P plated Cu substrates with the help of no-clean paste flux. The reflow was done at 250°C for 60 sec before cooling to room temperature in an infrared (IR) reflow oven (ESSEMTEC RO-06E). The multilayered Sn-3.5Ag/electroless Ni-P/Cu substrates were cut into a number of small reaction samples of area around 10 mm × 10 mm with the help of a diamond saw. Figure 1a shows the schematic diagram of the Sn-3.5Ag/electroless Ni-P/Cu sample used for the interfacial study. To prepare the tensile testing samples, two pieces of electroless Ni-P coated 6-mm-thick Cu substrates were joined together with Sn-3.5Ag with the same reflow process. A uniform thickness of solder layer was maintained between the Cu plates by using an alumina spacer of 650-μm thickness. The joined plates were cut, along the plate thickness direction, into a number of small samples of area around 600 μm × 650 μm with the help of a diamond saw. Figure 1b shows the schematic diagram of multilayered Cu/electroless Ni-P/Sn-3.5Ag/electroless Ni-P/Cu sample used for tensile testing.

Multiple reflows of 2, 5, 10, 15, 20, and 30 cycles were performed; each reflow followed the same

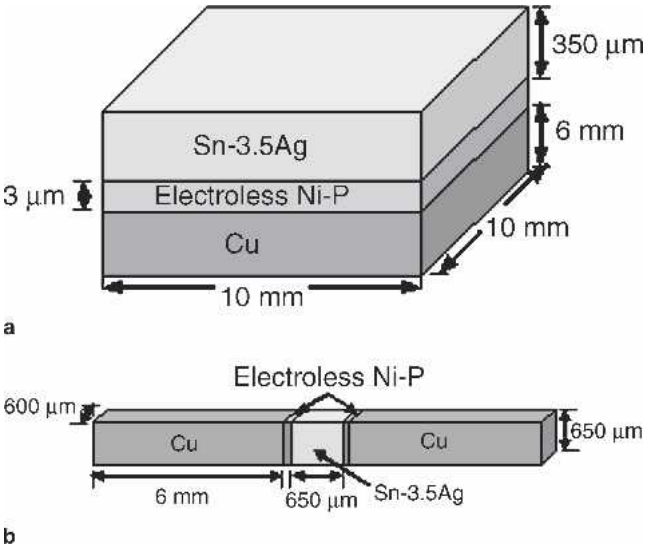

Fig. 1. Schematic diagram of test samples used for (a) interfacial study and (b) tensile testing.

temperature profile as the one used during sample preparation. A tensile test of the solder joints was performed using an INSTRON 5567 tensile tester. Five samples from each reflow condition were tested. The tensile test was done at room temperature with a constant crosshead speed of 0.05 mm/min. to a complete fracture. A JEOL JSM-6360A (Japan Electron Optics Ltd., Tokyo) scanning electron microscope (SEM) was used for interfacial microstructure analysis. For the cross-sectional SEM, the samples were cold mounted in epoxy and polished down to 1-μm finish using diamond paste. After polishing, solder etching was carried out to reveal the microstructure. Etching was done with 4 vol.% hydrochloric acid for a few seconds. Energy-dispersive x-ray (EDX) spectroscopy was performed in the SEM to analyze the chemical composition of interfacial compounds.

RESULTS AND DISCUSSION

Interfacial Microstructure Analysis

Figure 2 shows the interfacial microstructure of as-prepared samples. In all three types of as-prepared samples, two distinct compound layers were observed at the electroless Ni-P/Sn-3.5Ag interface. The light gray layer was of Ni_3Sn_4 intermetallic and the relatively thinner continuous dark gray layer formed between Ni_3Sn_4 and electroless Ni-P layers mainly consisted of Ni_3P compound. From previous electroless Ni-P/solder interfacial studies,[10,14] it is known that during interfacial reactions, Ni diffuses toward the solder side while Sn diffuses toward the electroless Ni-P side forming Ni_3Sn_4 intermetallic at the electroless Ni-P/solder interface. Owing to the depletion of Ni from electroless Ni-P, phosphorus atoms are left behind in the Ni-P layer. Continuous reactions between electroless Ni-P and solder cause large depletion of Ni from the electroless Ni-P layer. Consequently, there is an accumulation of P atoms at the interface between

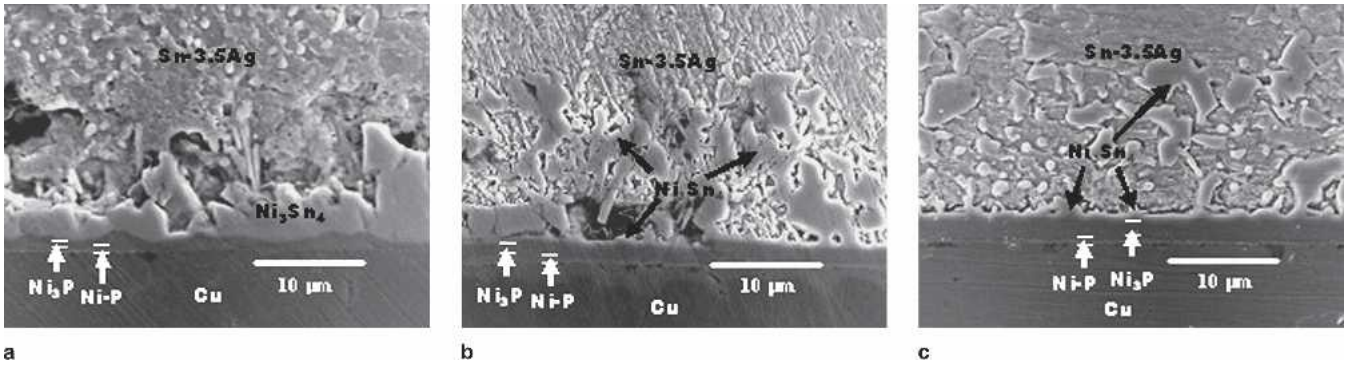

Fig. 2. Interfacial microstructures of as-prepared reaction samples having electroless Ni-P layers with (a) low (6.1 wt.%), (b) medium (8.8 wt.%), and (c) high (12.3 wt.%) P content.

electroless Ni-P and Ni_3Sn_4, resulting in the crystallization or transformation of electroless Ni-P layer into higher P content Ni-P (Ni_3P) layer.[5]

Comparing Fig. 2a through c, it is apparent that the electroless Ni-P layer in the low P sample was thinner than those in the higher P samples. This shows that electroless Ni-P UBM with low P was consumed more rapidly by Sn to form Ni_3Sn_4. Lower P content of electroless Ni-P layers results in a higher concentration gradient of Ni from the electroless Ni-P to the solder. This, in turn, allows faster Ni diffusion to the solder to form Ni_3Sn_4 and thus faster consumption of electroless Ni-P UBM. This finding is in agreement with the study by Sohn et al.[13] on the interfacial reaction between pure Sn and electroless Ni-P layers with different P contents. They observed that the thickness of Ni_3Sn_4 intermetallics increases; or, in other words, consumption of electroless Ni-P UBM increases with decreasing P content in the electroless Ni-P layer.

In this study, the Ni_3P layer that grew between electroless Ni-P and Ni_3Sn_4 layers was found to be the thinnest in the low P sample. A similar phenomenon has also been reported in previous interfacial studies between electroless Ni-P and different solders.[11–13] Sohn et al.[13] demonstrated differential scanning calorimetric analyses of electroless Ni-P layers with different P contents. It was reported that the crystallization temperature of electroless Ni-P decreases while the heat of crystallization increases with increasing P content in the electroless Ni-P layer. The experiment shows that the driving force for electroless Ni-P to transform into crystalline Ni_3P phase increases with increasing P content. During reflow, when enough thermal energy is provided, the thickness of the Ni_3P layer will be determined by the P content in the Ni-P coating. Stochiometrically, a higher P-containing sample will form thicker Ni_3P compared to a lower P sample. Following the same argument, a higher P-containing sample will form a smaller amount of Ni_3Sn_4 compared to a lower P-containing sample.

From Fig. 2, it is noticed that in the medium and high P samples, most of the Ni_3Sn_4 intermetallic compound spalled off into the solder, leaving behind a thin layer of Ni_3Sn_4 adhered to the reaction interface. The spallation of Ni_3Sn_4 intermetallic during electroless Ni-P/solder interfacial reactions has also been reported by Sohn et al.[16,18] Besides P content, other factors, such as solder composition and solder deposition method, have also been studied.[16,18] While some reports attributed the reason for the spallation to the existence of P-rich layer, Chen et al.[15] reported Ni_3Sn_4 spallation on pure Ni foils after long time reflow reaction. It is interesting to notice that for both Ni-P and pure Ni, there is always a layer of Ni_3Sn_4 that stays adhered to the remaining metallization underneath. This is quite different from the Cu-Sn IMC spallation,[1] where spallation only occurs when Cu metallization is fully consumed by reaction. The exact reason for Ni_3Sn_4 IMC spallation still needs more work for clarification. For the time being, we feel it could be caused by the joint action of multiple factors such solder composition, metallization composition, surface wetting condition, flux chemistry, interface stresses, etc. Fortunately, as will be illustrated later in this paper, Ni_3Sn_4 spallation does not seem to affect the joint strength before the metallization is fully reacted away.

Figure 3 shows the interfacial microstructure of the reaction samples subjected to five reflows. As compared to the as-prepared samples, it is apparent that the Ni_3Sn_4 intermetallics in all three reflowed samples grew further with the number of reflows, and thus, the electroless Ni-P layers became thinner as the reaction between Ni and Sn continued. It is worth noting that the electroless Ni-P UBM in the low P sample was completely consumed after five reflows. The thin dark Ni_3P layer was no longer continuous, compared with the as-prepared sample shown in Fig. 2a. Instead, at many locations, it transformed into a ternary Ni-Sn-P layer, which opened the channels for Sn to diffuse into the Cu substrate and for Cu to diffuse into the Ni_3Sn_4 layer. The diffusion of Sn and Cu through the "leaky" Ni_3P and Ni-Sn-P layers resulted in the formation of Ni-Cu-Sn and Cu-Sn intermetallics and a layer of voids at the Ni-Cu-Sn/Cu-Sn interface, as shown in Fig. 3a. No such formation of Ni-Cu-Sn and Cu-Sn intermetallics and layer of voids was observed in the samples with medium and high P electroless Ni-P UBM (Fig. 3b and c). This observation can be

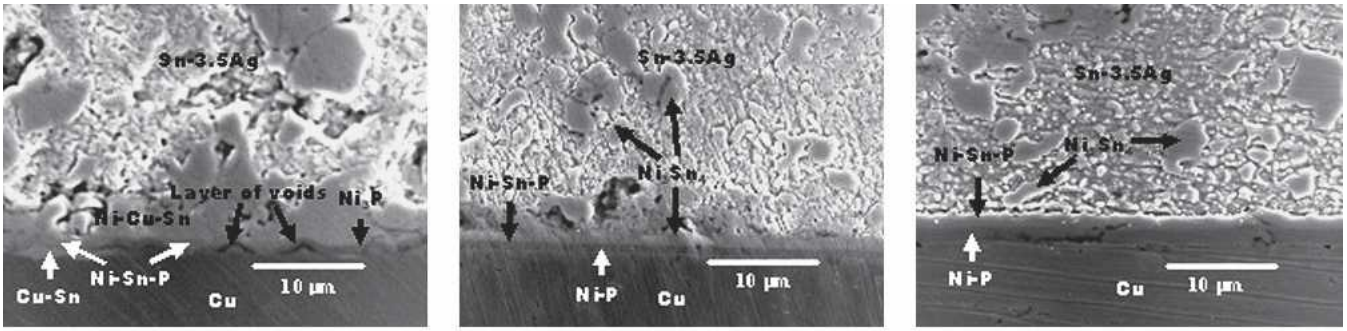

a b c

Fig. 3. Interfacial microstructures of the reaction samples having electroless Ni-P layers with (a) low (6.1 wt.%), (b) medium (8.8 wt.%), and (c) high (12.3 wt.%) P content after five reflows.

explained by considering the lower consumption of higher P-containing electroless Ni-P UBM. The exact phases of the Ni-Cu-Sn and Cu-Sn IMCs were reported elsewhere.[9,10] As discussed previously, the Ni_3P layer grows thicker with increasing P content in the electroless Ni-P UBM. The thicker Ni_3P layer will slow the Ni diffusion from electroless Ni-P to the Ni_3Sn_4/Ni_3P interface due to the lower concentration gradient of Ni, and consequently, consumption of electroless Ni-P UBM will be slowed. This is the reason there was still a continuous electroless Ni-P layer remaining in the medium and high P samples after five reflows. This remaining electroless Ni-P layer prevented the formation of Ni-Cu-Sn and Cu-Sn intermetallics and layer of voids.[9,10]

The interfacial microstructures of the three Ni-P samples after 20 reflows are depicted in Fig. 4. All samples contained some features in common. Quite a large amount of Ni-Cu-Sn and Cu-Sn intermetallics was present at the interface along with a thick layer of voids. Moreover, no trace of electroless Ni-P was found in all the samples and there was no more Ni_3Sn_4 present at the interface. The apparent distinction between the three samples was that the Ni-Cu-Sn and Cu-Sn intermetallics formed in low P sample were the thinnest among all the samples. The presence of thick layers of Ni-Cu-Sn and Cu-Sn intermetallics in the samples with medium and high P electroless Ni-P UBM can be understood to be due to the Ni_3Sn_4 spallation, which occurred typically in the medium and high P samples. Kumar et al.[9,10] reported that in the Cu/Ni-P/Sn-3.5Ag solder joint, after complete transformation of electroless Ni-P layer into Ni_3P layer, Cu starts diffusing out from the Cu substrate to form Ni-Cu-Sn intermetallics at the Ni_3Sn_4/Ni-Sn-P interface. The depletion of Cu from the Cu substrate results in the formation of a layer of voids at the Ni_3P/Cu interface, and eventually, Sn coming from the solder reaches the Cu substrate and forms Cu-Sn intermetallics at the Ni-Sn-P/Cu interface. Thus, in the case of medium and high P samples, owing to the Ni_3Sn_4 spallation, the Cu-Sn and Ni-Cu-Sn intermetallic formation is expected to be rapid because the Ni_3Sn_4 spallation shortens the Sn and Cu diffusion paths through the remaining compound layers.

Tensile Strength and Fractographic Analysis

Figure 5 shows the variation in the average tensile strengths of low, medium, and high P samples as the samples underwent multiple reflows, while Table I lists the average tensile strength values. From Fig. 5, it is obvious that the tensile strength of all three types of samples (low, medium, and high P) decreases with the increasing number of reflows. All three types of samples showed similar strength up to five reflows. However, beyond five reflows, the strength of medium and high P samples decreased

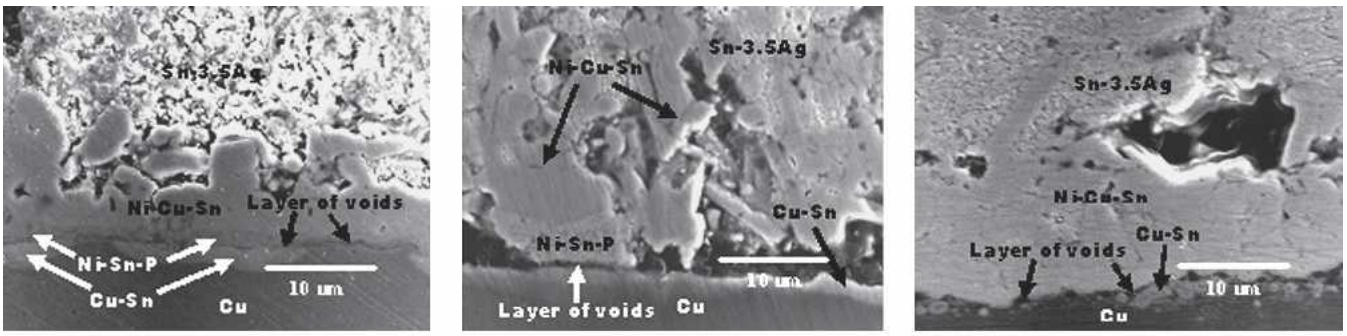

a b c

Fig. 4. Interfacial microstructures of the samples having electroless Ni-P layers with (a) low (6.1 wt.%), (b) medium (8.8 wt.%), and (c) high (12.3 wt.%) P content after 20 reflows.

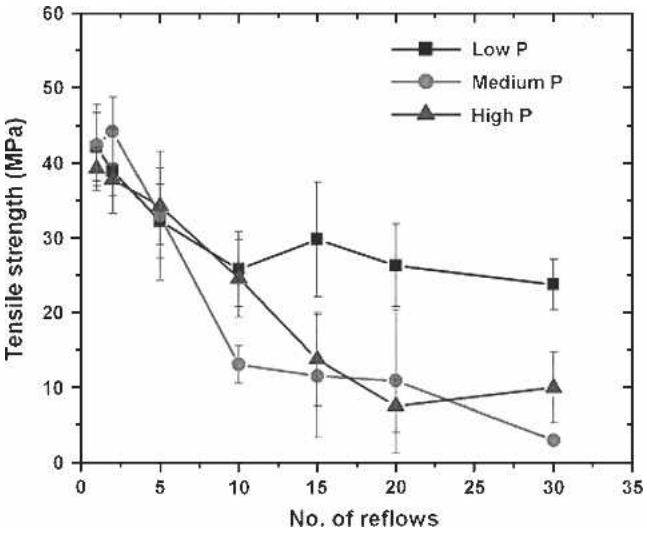

Fig. 5. The tensile strength of low, medium, and high P samples after multiple reflows.

Table I. Average Tensile Strength of Cu/Electroless Ni-P/Sn-3.5Ag Solder Joints after Multiple Reflows

Number of Reflows	Average Tensile Strength (MPa)		
	Low P	Medium P	High P
1	42.13	42.38	39.23
2	38.96	44.22	37.81
5	32.22	32.94	34.22
10	25.79	18.04	24.56
15	29.76	11.51	13.73
20	26.28	10.89	7.49
30	23.75	2.99	9.95

rapidly, while the strength of low P sample stabilized and remained nearly unchanged. The strengths of medium and high P samples were observed to be comparable to each other after 10 reflows. To sum up, low P samples exhibited the highest tensile strength among all after multiple reflows. In other words, the degradation in strength was the lowest in the case of the low P sample.

To understand the reasons for degradation in the tensile strength of Cu/electroless Ni-P/Sn-3.5Ag solder joints having different P containing electroless Ni-P layers, in-depth studies of fracture surfaces and fracture path were carried out. Figures 6 and 7, respectively, show the typical fracture path and fracture surfaces occurring in the multiple reflowed samples. A general trend was observed in the fracture surfaces and fracture path of the samples having different P containing electroless Ni-P layers. For up to two reflows, in all three types of samples, the fracture path was entirely inside the solder (Figs. 6a and 7a). However, as the number of reflows increased, the fracture path shifted from inside the bulk solder to the reaction interfaces between the solder and Cu substrate (Figs. 6b and 7b). This indicates that in the samples reflowed more than two times, the cohesive strength of the compounds formed at the Cu/electroless Ni-P/Sn-3.5Ag interfaces and their adhesive strengths with both the Cu substrate and solder were much lower than the cohesive strength of the solder itself. From Figs. 6a and 7a, it is also apparent that the failure mode was ductile in the samples reflowed up to two times. The necking in the solder (Fig. 6a) clearly indicates that the solder experienced quite a large amount of plastic deformation before fracture. However, as shown in Figs. 6b and 7b, with an increased number of reflows, the appearance of fracture surface changed macroscopically from a rough to nearly flat surface; in other words, the failure mode changed from ductile to brittle.

Figure 8 is the SEM images of fracture surfaces of the medium P samples reflowed for multiple times. The figure shows a clear transition in the fracture surfaces. In the sample reflowed for five times, fracture surfaces were at the Cu/Ni_3P and Ni_3P/Ni-Cu-Sn interfaces (Fig. 8a and b), which shifted to the Ni-Sn-P/Cu and Ni-Sn-P/Cu-Sn interfaces with the increase in reflow cycles (Fig. 8c and d). Finally,

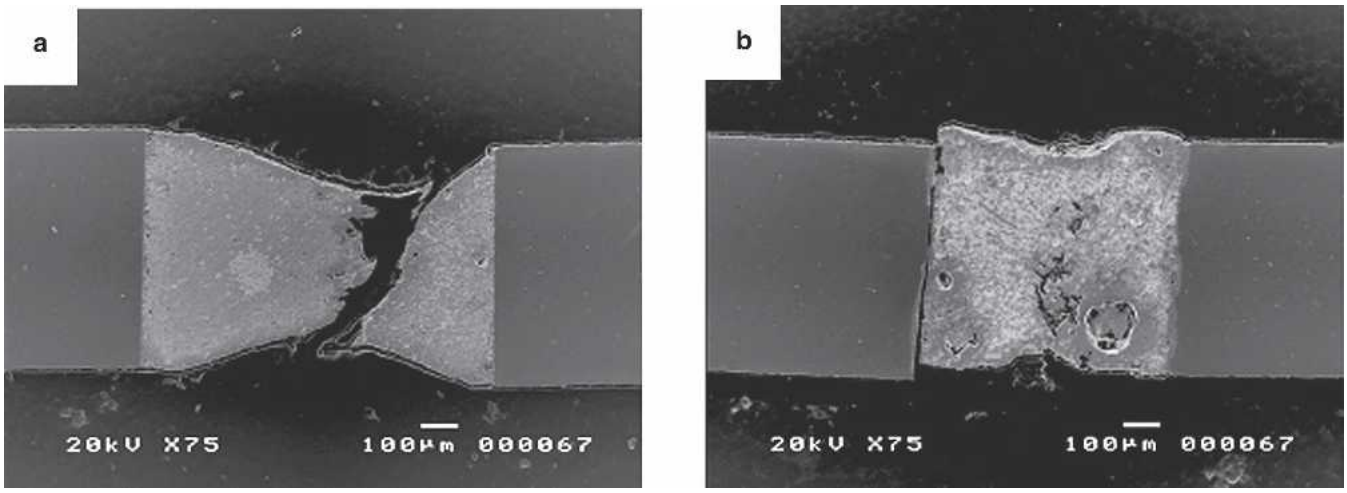

Fig. 6. Fracture path in low P sample (a) after 2 reflows and (b) after 20 reflows, showing the transition from ductile to brittle failure as the number of reflows increased.

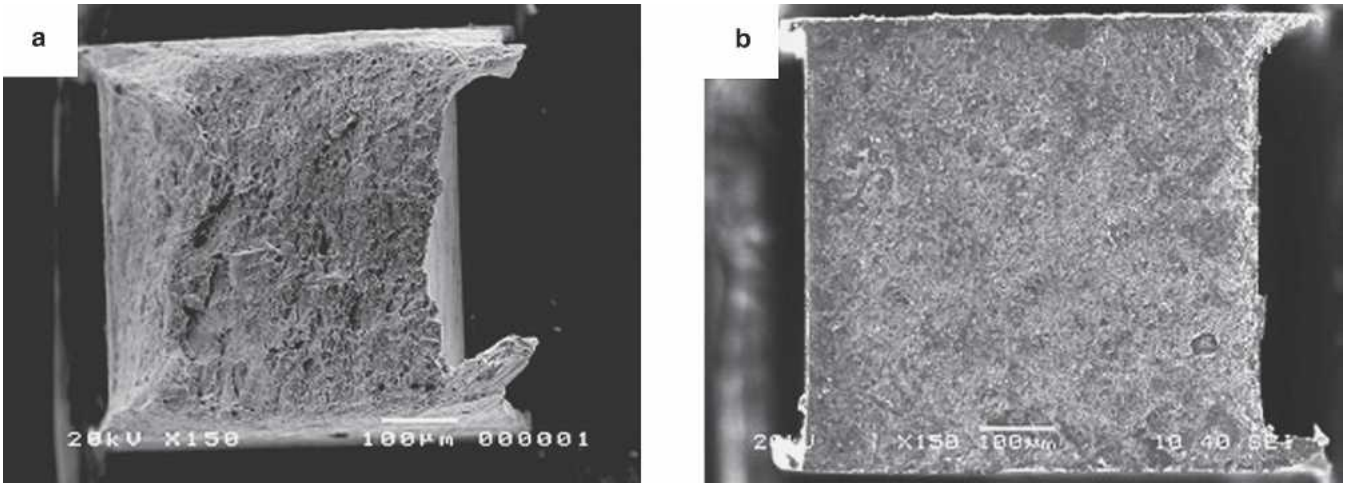

Fig. 7. Fracture surfaces of high P sample (a) after 2 reflows and (b) after 20 reflows, showing the transition from ductile to brittle failure as the number of reflows increased.

fracture surfaces were at the Ni-Sn-P/Cu-Sn interface owing to the thick Cu-Sn intermetallics on the Cu substrate. Fig. 8e and f identify the fracture path at such interface. The thick Cu-Sn intermetallics on the Cu substrate are confirmed by the SEM image of the fracture path, shown in Fig. 9.

Kumar et al.[17,19] have shown that in the case of Cu/electroless Ni-P/solder joint, the Ni_3P/Cu and Ni-Sn-P/Cu interfaces are more prone to fracture due to the formation of a layer of voids at these interfaces. The layer of voids at the Ni_3P/Cu interface forms after complete transformation of electroless Ni-P layer into Ni_3P layer and due to the depletion of Cu from the Cu substrate through the Ni_3P layer, and the layer of voids remains at the reaction interface even after formation of Ni-Sn-P and Cu-Sn compounds.[10] In the current study, a similar layer of voids was observed at the reaction interface at and beyond five reflows (Figs. 3 and 4), which caused the facture to occur at the Ni_3P/Cu interface (Fig. 8a and b). The growth of Ni-Sn-P and Cu-Sn compounds at the Ni_3P/Cu interface changed the appearance of fracture surfaces (Fig. 8b, c, d, and e) and severely decreased the tensile strength (Fig. 5). Thus, the decrease in tensile strength during multiple reflows can be understood to be due to the growth of Ni-Sn-P and Cu-Sn compounds and the formation of a layer of voids between the solder and Cu substrate.

Although the cause of degradation in tensile strength of all three types of reflowed samples is quite clear, the cause of the relatively lower decrease in tensile strength of the low P sample has to be understood as well. As discussed in the previous section, owing to the low intermetallic spalling, the growth of Cu-Sn IMCs in the low P samples was very low as compared to that of the medium and high P samples. Because the growth of Cu-Sn IMCs severely deteriorated the tensile strength of solder joints (Figs. 5, 8, and 9), the lower decrease in tensile strength of low P samples is attributed to the low growth rate of Cu-Sn IMCs. Despite that, the voids have been formed at some locations at the Ni-Sn-P/Cu-Sn interface in the low P sample after five reflows (Fig. 3a); their effect on the tensile strength is almost negligible because at five reflows tensile strength for all three P-containing samples is very similar (Fig. 5). The reason could be that both the size and density of the voids in the low P samples are not high enough to influence the joint strength. We further noticed that these voids only appeared at some locations and were not continuous (Fig. 3a). Fractographic observation shows that the fracture path is at mixed Cu/Ni_3P and Ni_3P/Ni-Cu-Sn interfaces. This implies that these interfaces were weaker than the voided ones, but discontinuous Ni-Sn-P/Cu-Sn interface for five times reflowed low P samples.

An interesting point to observe when studying the strength degradation of all three types of samples is the fracture surface. Unlike the ones for medium and high P samples, where mixed fracture along the Cu/Ni_3P and Ni_3P/Ni-Cu-Sn interface occurred only in a small number of reflows (Fig. 8), in the low P sample, fracture occurred at the mixed interfaces even after 20 cycles of reflow (Fig. 10). This prolonged stay of this mixed fracture could be the reason for no significant drop in tensile strength (Fig. 5). We tried to determine the cause for this mixed facture in the case of low P samples. From interfacial analysis, it was found that in the low P samples, mixed fracture occurred due to the uneven growth of the interface compounds, as shown in Figs. 3 and 4. The cause for uneven compound growth in the low P samples is not very clear at this moment. We believe that the size of Ni_3P grains and grain boundaries plays an important role in the uneven growth of interfacial compounds and further work is needed to understand this phenomenon. Nevertheless, it is apparent that the uneven growth (which means at some location the interface reaction is much slower) will prolong the time that voids at the interface collapse into a continuous layer. As a result, the

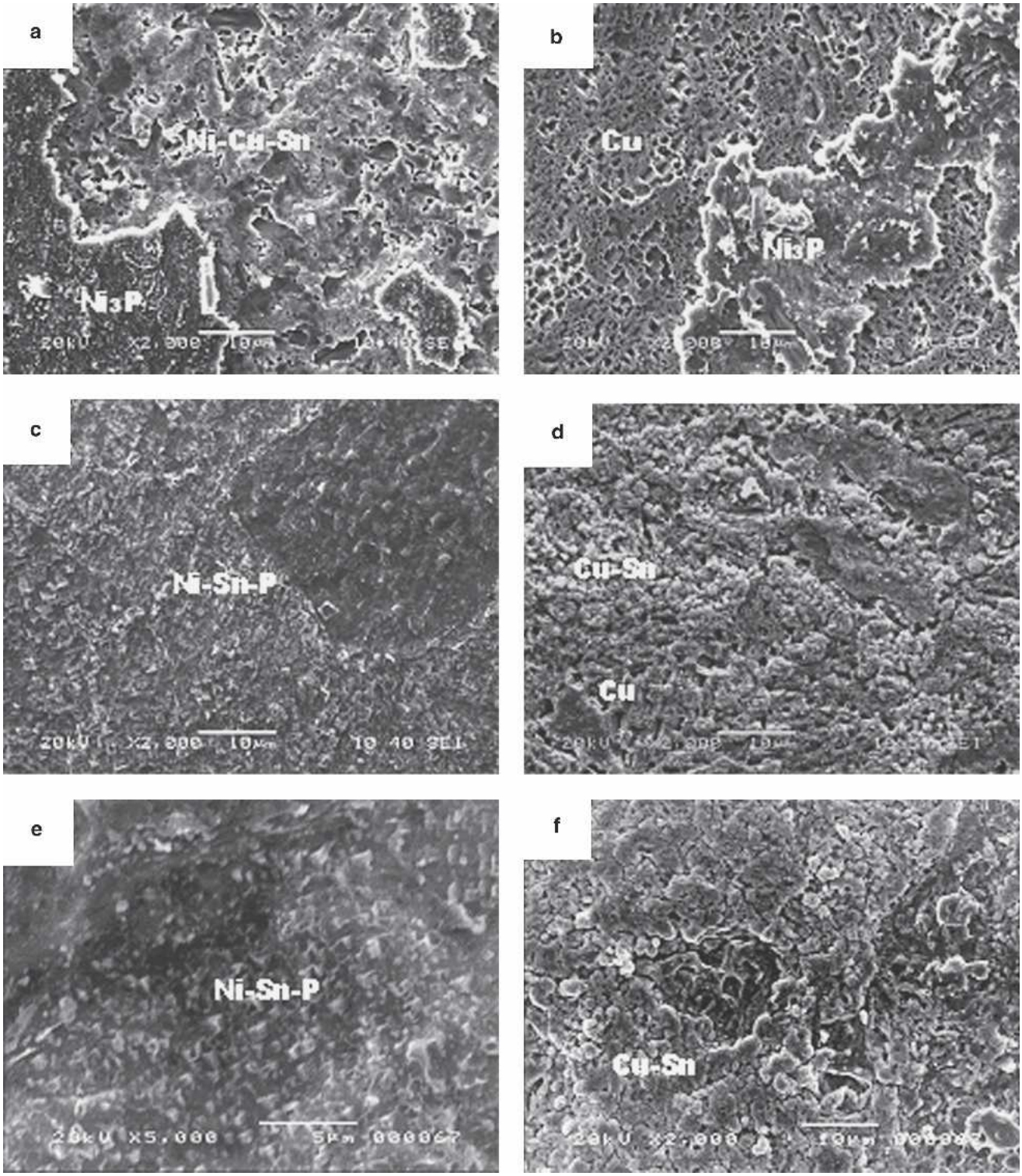

Fig. 8. Fracture surfaces of medium P samples after reflow for (a) 5 cycles (solder side), (b) 5 cycles (Cu substrate side), (c) 15 cycles (solder side), (d) 15 cycles (Cu substrate side), (e) 30 cycles (solder side), and (f) 30 cycles (Cu substrate side).

residual strength of the interface remains relatively higher even after a large number of reflows.

CONCLUSIONS

From the present study, it was found that the P content of the electroless Ni-P layer influences the interfacial microstructure and mechanical strength of Cu/electroless Ni-P/Sn-3.5Ag solder joints. Low P samples exhibited the highest joint strength among all, with little drop in tensile strength. The strengths of medium and high P samples decreased rapidly with the increase in reflow cycles. In the early stage, the low P electroless Ni-P layer consumed

more rapidly by its reaction with Sn due to the higher concentration gradient of Ni from electroless Ni-P layer to solder. However, the Ni_3Sn_4 intermetallic compound in the low P sample was found to remain at the interface. In contrast, Ni_3Sn_4 formed at the interface of medium and high P samples mostly spalled into the molten solder, and eventually the remaining electroless Ni-P layer consumed rapidly as the reflow cycles progressed. Although Ni_3Sn_4 spallation was not found to influence the solder joint strength directly, it shortened the Sn diffusion path from the solder through the remaining compound layers, and consequently Ni-Cu-Sn and Cu-Sn intermetallics grew rapidly with the number of reflows. The thick Ni-Cu-Sn and Cu-Sn intermetallics deteriorated the tensile strength of medium and high P samples severely due to void formation at the interface. Therefore, low P electroless Ni-P is the best electroless Ni-P UBM against multiple reflows because of its high solder joint strength and low intermetallic spalling and growth.

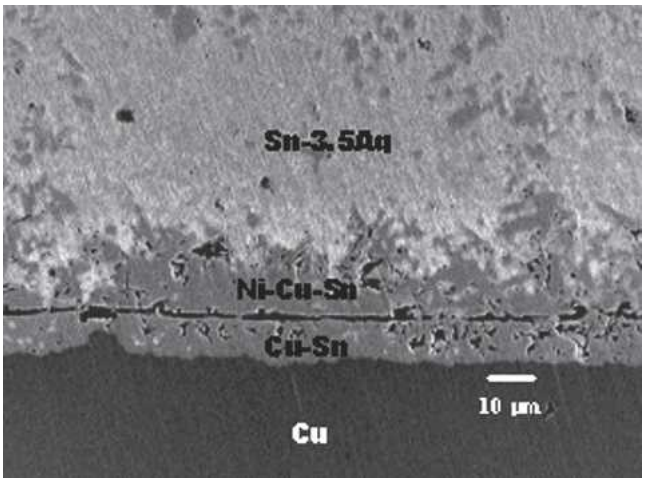

Fig. 9. SEM image of fracture path in the medium P sample reflowed for 30 cycles, showing thick Cu-Sn intermetallics on the Cu substrate.

ACKNOWLEDGEMENTS

This work was supported by Research Grant No. RG19/00 from Nanyang Technological University, Singapore, and JT ARC 2/03 from MOE/A*Star, Singapore.

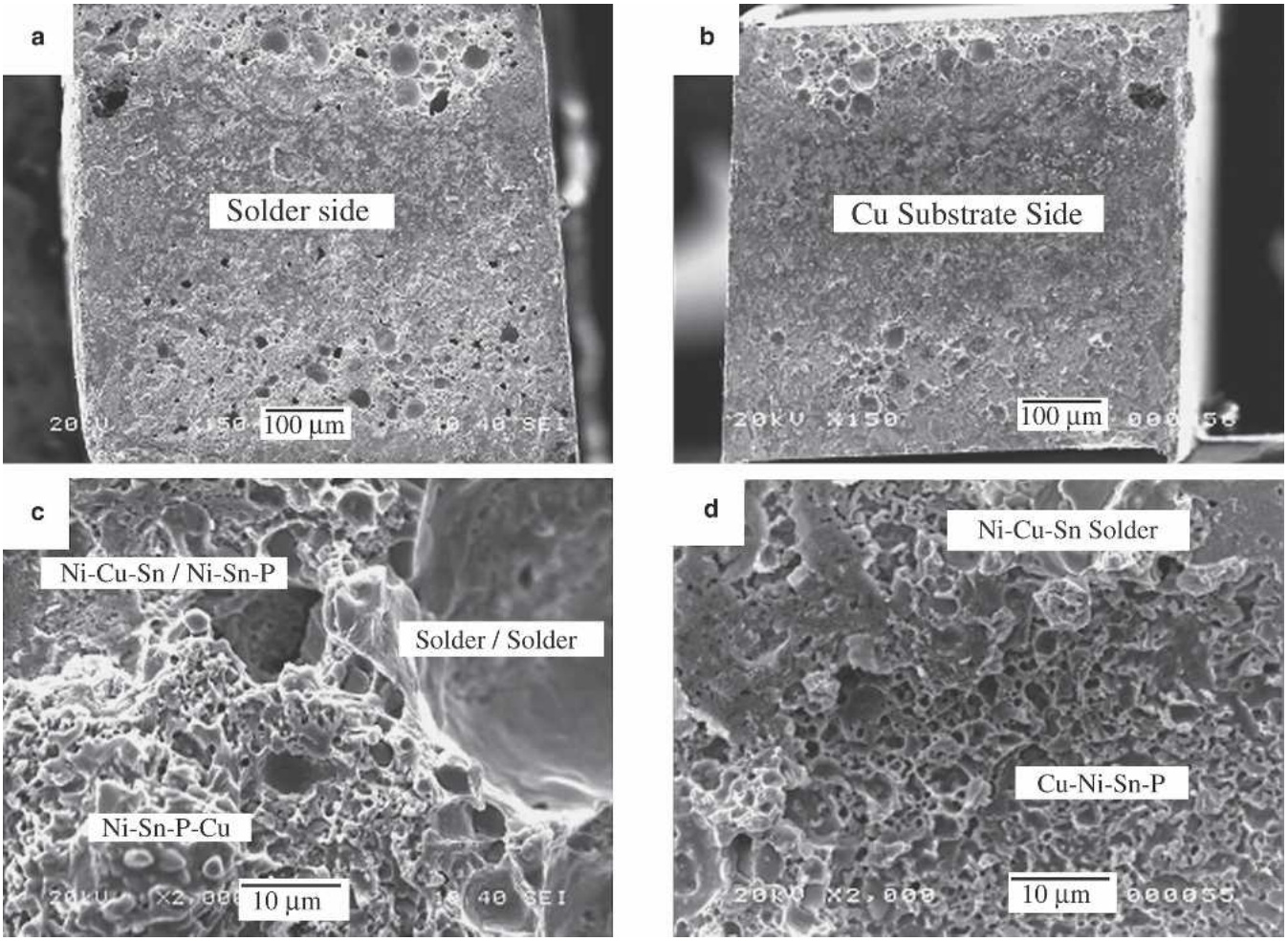

Fig. 10. Fracture surfaces of low P sample after 20 reflows: (a) solder side; (b) Cu substrate side; (c) magnified image of solder side; and (d) magnified image of Cu substrate side, showing that fracture occurred at mixed solder/solder, solder/Ni-Cn-Sn, Ni-Cu-Sn/Ni-Sn-P, and Ni-Sn-P/Cu interfaces.

REFERENCES

1. A.A. Liu, H.K. Kim, K.N. Tu, and P.A. Totta, *J. Appl. Phys.* 80, 2774 (1996).
2. J.W. Jang, L.N. Ramanathan, J.K. Lin, and D.R. Frear, *J. Appl. Phys.* 95, 8286 (2004).
3. K.N. Tu and K. Zeng, *Mater. Sci. Eng. R* 34, 1 (2001).
4. K.L. Lin and Y.C. Liu, *IEEE Trans. Adv. Packaging* 22, 568 (1999).
5. J.W. Jang, P.G. Kim, K.N. Tu, D.R. Frear, and P. Thompson, *J. Appl. Phys.* 85, 8456 (1999).
6. G.O. Mallory and J.B. Hajdu, *Electroless Plating: Fundamentals and Applications* (Orlando, FL: American Electroplaters and Surface Finishers Society, 1990), ch. 4.
7. Y.C. Chen, P.L. Tu, C.W. Tang, K.C. Hung, and K.L. Joseph, *IEEE Trans. Adv. Packaging* 24, 25 (2001).
8. M. He, Z. Chen, and G. Qi, *Acta Mater.* 52, 2047 (2004).
9. A. Kumar, M. He, and Z. Chen, *Surf. Coating Technol.* 198, 283 (2005).
10. A. Kumar, Z. Chen, S. Mhaisalkar, C.C. Wong, P.S. Teo, and V. Kripesh, *Thin Solid Films* 504, 410 (2006).
11. Y. Chonan, T. Komiyama, J. Onuki, R. Urao, T. Kimura, and T. Nagano, *Mater. Trans.* 43, 1840 (2002).
12. M.O. Alam, Y.C. Chan, and K.N. Tu, *J. Appl. Phys.* 94, 4108 (2003).
13. Y.C. Sohn, J. Yu, S.K. Kang, D.Y. Shih, and W.K. Choi, *J. Electron. Mater.* 33, 790 (2004).
14. C.Y. Lee and K.L. Lin, *Thin Solid Films* 249, 201 (1994).
15. Z. Chen, M. He, and G. Qi, *J. Electron. Mater.* 33, 1465 (2004).
16. Y.C. Sohn, J. Yu, S.K. Kang, D.Y. Shih, and T.Y. Lee, *J. Mater. Res.* 19, 2428 (2004).
17. A. Kumar and Z. Chen, *Proc. 7th Electronic Packaging and Technology Conf.* (Piscataway, NJ: IEEE, 2005), p. 873.
18. Y.C. Sohn, J. Yu, S.K. Kang, D.Y. Shih, and T.Y. Lee, *Electronic Components and Technology Conf.* (2005).
19. A. Kumar and Z. Chen, *Mater. Sci. Eng. A*, in press.